Contributions of floodplain stratigraphy and evolution to the spatial patterns of groundwater arsenic in Araihazar, Bangladesh

Beth Weinman†
Steven L. Goodbred Jr.
Earth and Environmental Sciences, Vanderbilt University, Nashville, Tennessee 37235, USA

Yan Zheng
Lamont-Doherty Earth Observatory of Columbia University, Palisades, New York 10964, USA
Queens College, City University of New York, Flushing, New York 11367, USA

Zahid Aziz
Michael Steckler
Alexander van Geen
Lamont-Doherty Earth Observatory of Columbia University, Palisades, New York 10964, USA

Ashok K. Singhvi
Yogesh Chand Nagar
Physical Research Laboratory, Navrangpura, Ahmedabad, India 380 009

ABSTRACT

Extreme spatial heterogeneity has emerged as a salient characteristic of groundwater arsenic in many complex fluviodeltaic environments. Here we examine patterns of arsenic heterogeneity in the shallow (<23 m) groundwaters of a well-studied floodplain setting in Araihazar, Bangladesh. Ninety-five augers and 200 shallow wells sampled at spacings of 10^1–10^3 m in the 25 km^2 area indicate that the concentration of arsenic in shallow groundwater largely varies with the grain size, thickness, and distribution of fine-grained (<63 μm) sediments that overlie buried aquifer sands. The overall pattern shows that lower arsenic concentrations are typically found where aquifer sands outcrop at or near the surface, whereas higher arsenic levels typically underlie, or are adjacent to thicker, fine-grained deposits. Furthermore, chronostratigraphic reconstructions of aquifer sediments indicate that sediment distribution, and consequently the patterning of dissolved arsenic, is readily explained in the context of local river history and floodplain development within the past 1000 yr. An important implication is that complex patterns of groundwater arsenic in afflicted fluviodeltaic settings can be better understood through reconstructions of local aquifer history. This finding is especially relevant because the village and tube-well locations are closely linked with surface landforms such as former levees and bars. An additional and worrisome finding is that the artificial filling of villages to protect from flooding can mimic the natural fine-grained stratigraphy commonly associated with high concentrations of arsenic.

Keywords: arsenic, groundwater, Bangladesh, floodplain, stratigraphy.

INTRODUCTION

The occurrence of arsenic in the alluvial aquifers of many fluvial and deltaic systems has become a well-known tragedy affecting at least 100 million people in South and Southeast Asia (e.g., British Geological Survey/Department of Public Health Engineering [BGS/DPHE] report, 2001; Berg et al., 2001; Liu et al., 2004; McArthur et al., 2004). After nearly a decade of research, it has become increasingly evident that distinct spatial patterns in arsenic contamination exist. The Ganges-Brahmaputra and Red River delta complexes exhibit general downriver enrichment trends in tube-well arsenic (BGS/DPHE, 2001; Berg et al., 2001), and similar downstream trends occur in medium-to-small fluvial drainages of West Bengal and the alluvial fans of Taiwan and Inner Mongolia (Smedley et al., 2003; Liu et al., 2004; Sengupta et al., 2004).

To some extent, such regional trends (10^1–10^2 km) in dissolved arsenic distribution can be explained by geological properties. In Bangladesh and West Bengal, Tertiary and Pleistocene uplands remain relatively unaffected by arsenic, whereas Holocene floodplains and delta plains typically have moderate (40%–60% of tube wells >10 μg/L) to strong enrichments (>80% of tube wells >10 μg/L) of shallow groundwater arsenic (Acharyya et al., 2000; BGS/DPHE, 2001; Ahmed et al., 2004; Ravenscroft et al., 2005). Even within the frequently arsenic-rich Holocene aquifers, patterns of tube-well arsenic track large-scale (10^1 km) geologic and geomorphic features (Yu et al., 2003). Less well studied is the significant spatial structuring of arsenic heterogeneity observed within the few densely sampled, and thus better resolved, study areas investigated so far (e.g., 2–10 km spacing by BGS/DPHE, 2001, and <100–1000 m by van Geen et al., 2003). In the latter case, 50-fold differences in arsenic concentration were documented in wells located several meters apart and screened at the same depth (e.g., 7 versus 321 μg/L, van Geen et al., 2003).

To better understand how such heterogeneity develops, investigating aquifers over less regional scales would help test whether ground-

†E-mail: beth.weinman@vanderbilt.edu; phone: 615-322-2976; fax: 615-322-2138

GSA Bulletin; November/December 2008; v. 120; no. 11/12; p. 1567–1580; doi: 10.1130/B26209.1; 9 figures; 5 tables.

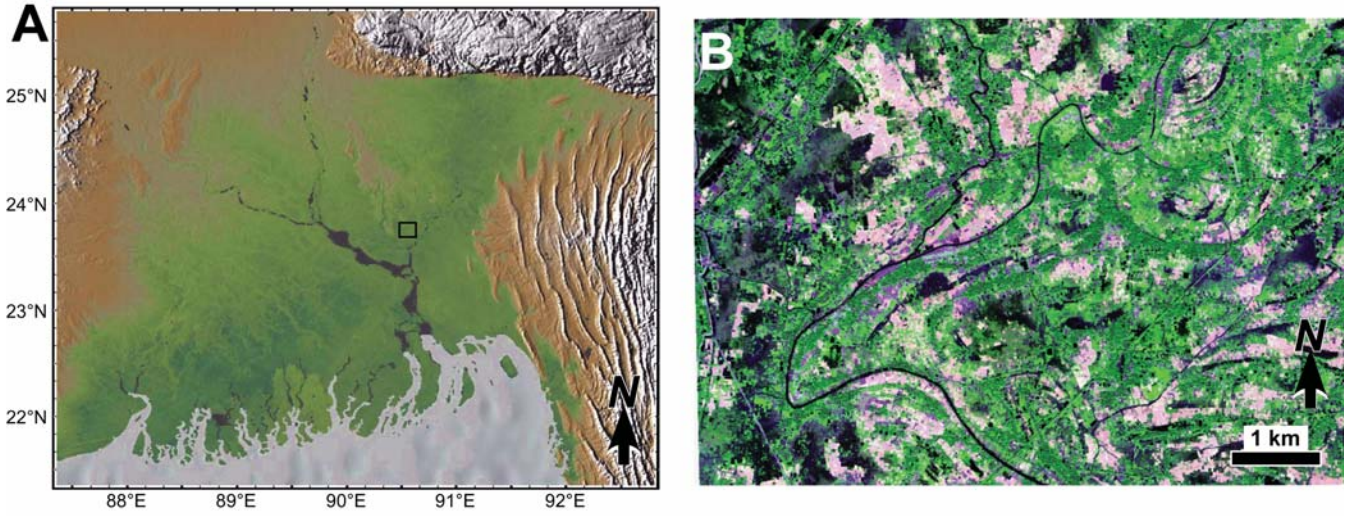

Figure 1. (A) Location of Araihazar study site in the mid-delta portion of Bangladesh on a nationwide map showing Araihazar's location (box) between the modern Meghna River to the east and the elevated Pleistocene-age Madhupur Terrace to the northwest. (B) Ikonos image of Araihazar, which shows complex floodplain morphology of the region.

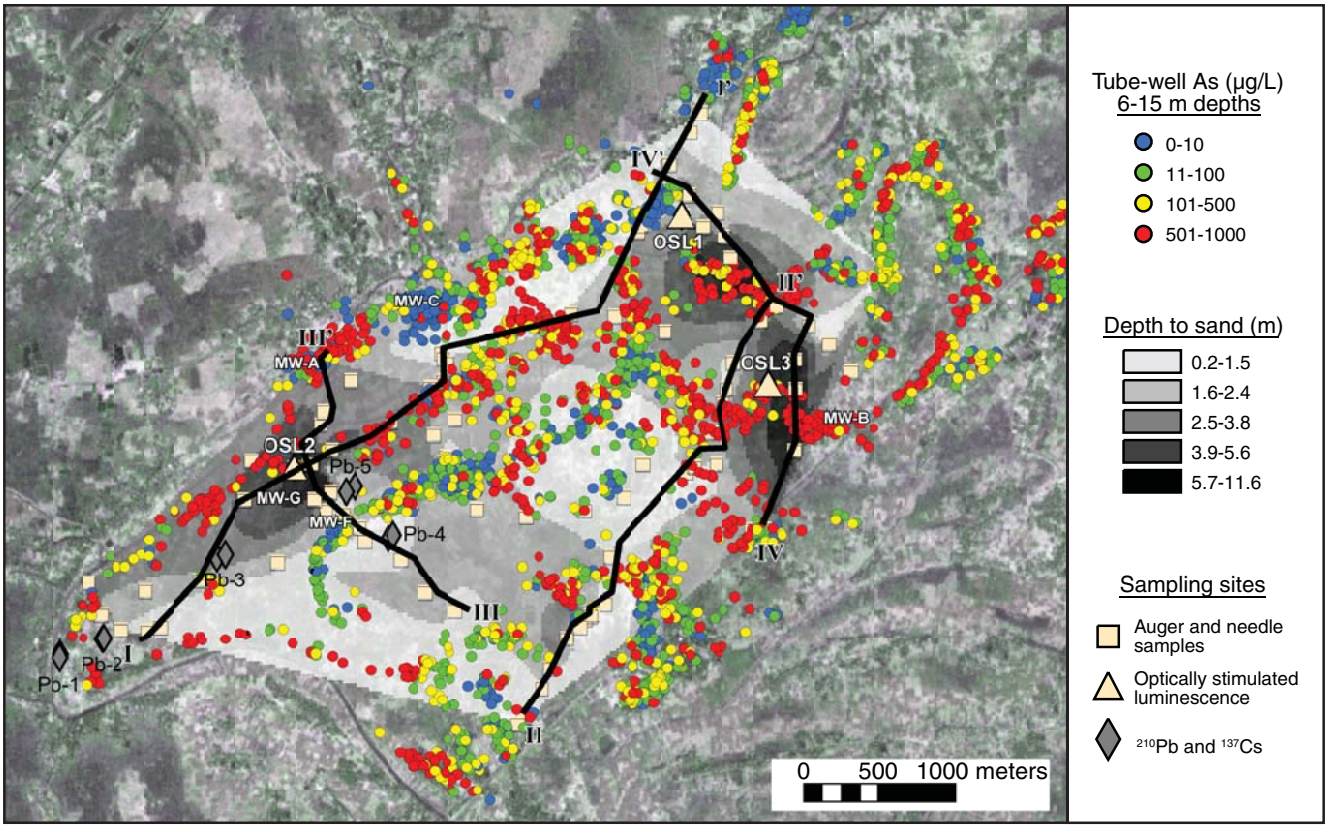

Figure 2. Site map showing color-scale values of shallow tube-well arsenic, grayscale depth-to-sand values, sediment sampling locations, and transect locations. Tube-well arsenic values from van Geen et al. (2003) are shown only for shallow wells at 6–15 m depth. Mean concentration of the 101–1000 category is 245 ± 122 µg/L. The interpolated depth-to-sand surface is shown in grayscale and classified by a natural Jenks method that minimizes squared deviations between data class means. Observed trends indicate generally lower arsenic concentrations coincident with shallowly buried aquifer sands, with concentrations increasing with depth of sand burial by muddy floodplain sediments. Sampling sites include sediment and stratigraphic data (squares) collected from hand augers and needle samples, location of sands dated by optically stimulated luminescence (OSL) (triangles), and floodplain accretion rates measured by ^{210}Pb and ^{137}Cs geochronology (diamonds). Villages with multi-well monitoring sites referred to in the text are depicted by MW-A, MW-B, MW-C, MW-F, and MW-G. Cross-section transects produced from these data, I–I′, II–II′, III–III′, and IV–IV′, are shown by heavy black lines and are results depicted in Figure 5.

water arsenic heterogeneity can be explained by local variations in aquifer stratigraphy. Several studies have already suggested a connection between arsenic enrichment and specific fluviodeltaic deposits, including peats, silts and clays, and reducing gray sands (e.g., McArthur et al., 2004; Bibi and Ishiga, 2006; Meharg et al., 2006; von Brömssen et al., 2007). However, it is unclear how these sedimentary units, and corresponding groundwater arsenic, are distributed beyond the immediate study sites. Thus, characterizing the types and continuity of shallow sedimentary deposits over tens to hundreds of meters is necessary (Sandberg et al., 2002) to understand why juxtaposing villages and tube wells have order-of-magnitude differences in groundwater arsenic. In the absence of well-constrained subsurface lithology, arsenic heterogeneity in these floodplain environments remains poorly constrained and is not explained by changes in local rainfall, groundwater levels, or major ion compositions (BGS/DPHE, 2001; Cheng et al., 2005; Dhar, 2006).

Thus, the goal of this work is to provide a fundamental framework on how landscape heterogeneity can contribute to the local arsenic variability observed in Bangladesh's groundwater. Studies by McArthur et al. (2004) and Horneman et al. (2004) suggest that different surficial deposits can control the distribution of arsenic in underlying shallow aquifers. This notion has been reinforced by a geophysical study by van Geen et al. (2006a) showing that variations in shallow-aquifer arsenic at scales <1 km within the Araihazar floodplain in Bangladesh are significantly correlated with electromagnetic conductivity of the top ~5–6 m of sediment. In the present paper, we explore the origin of this general relationship in terms of floodplain evolution by first correlating 10^3 m-scale distributions of groundwater arsenic to depositional patterns of modern and relict stream channels. We then show that fine-scale patterns (10^1–10^2 m) of groundwater arsenic are controlled by local fluvial subenvironments (e.g., meander bars and levees). Finally, we examine the potential effects of anthropogenic floodplain modification on arsenic concentrations. The hope is that the sedimentological framework observed from this investigation will help to understand fine-scale arsenic distributions and guide mitigation through the geological features that characterize fluviodeltaic sedimentary basins.

STUDY SITE

To test whether subsurface lithology and depositional differences can explain the shallow (<23 m) groundwater arsenic heterogeneity over distances of tens to thousands of meters, we chose to work in the 25-km^2 "*upazila*"of Araihazar, Bangladesh (90°37′E, 23°47′N). Similar to initial reports of localized arsenic variability in Chapai Nawabganj, Faridpur, and Lakshmipur by the British Geological Survey (BGS/DPHE, 2001, sampling density ~1 tube well per 7 km^2), a comprehensive 6000–tube-well survey conducted in Araihazar (van Geen et al., 2002, 2003) makes it a prime location for resolving the sedimentological and stratigraphical influence on arsenic in the shallow aquifer.

Geomorphically, Araihazar constitutes a complex floodplain setting, juxtaposed by two uplifted Pleistocene terraces and distally located ~10 km west of the current Meghna River (Fig. 1). More recently, Araihazar has been strongly influenced by the Brahmaputra River prior to its westward avulsion beginning ~150 yr ago (Fergusson, 1863). Within this largely abandoned fluvial setting, Araihazar's groundwater can vary over several meters in wells drilled to the same depth (van Geen et al., 2003). Such acute differences are not the focus of this study, but the general patterning of groundwater arsenic at scales of hundreds to thousands of meters is perhaps more relevant for water resource management because these are the distances at which community wells are typically distributed (van Geen et al., 2006b).

METHODS

To evaluate the effect of floodplain morphology on the pattern of arsenic concentrations in shallow groundwater, four primary coring transects were completed, consisting of 95 hand augers to depths of 5 m and 15 needle-sampler profiles to depths of 30 m (Fig. 2; see van Geen et al., 2004, for description of needle sampler). Site selection was based on surface-sediment conductivity measures using a Geonics EM-31 and the 6000–tube-well survey of shallow-aquifer arsenic concentrations (van Geen et al., 2006a). Sediment grain size was analyzed on 129 samples from 19 auger and 11 needle-sample profiles and, along with detailed field descriptions, was used to differentiate the major sedimentary facies comprising local floodplain environments. The sedimentary facies were placed into vertical stratigraphic successions compiled from auger and needle-sample data, as well as field notes. Resulting stratigraphic facies were identified on the basis of their dominant sediment type, unit thickness, and stacking patterns. The distribution of stratigraphic facies, along with a digital elevation model, radiometrically derived accretion rates, and luminescence dating, allowed for a reconstruction of the floodplain's geomorphic development. The floodplain-evolution model that emerged was then compared with arsenic distributions in ArcView-GIS (geographic information system) using a subset of 200 tube wells that are <15 m deep and located within 50 m of the auger transects (van Geen et al., 2003). Method details are available in the Appendix.

RESULTS

Floodplain Geology

Sedimentary and Stratigraphic Facies

Four major sedimentary facies (facies *i, ii, iii,* and *iv*), defined primarily by their silt content and gradual fining of the sand component, dominate the surficial floodplain deposits of Araihazar (Fig. 3). These facies include: (*i*) a well-sorted sand with ~85%–100% of the particles in the 100–500 μm size range and very little silt; (*ii*) a moderately well sorted silty fine sand with > 50% of the grains 63–250 μm, but locally grading to (ii_a) a clean, coarse silt; (*iii*) a poorly sorted mud with a 2:1 ratio of silt to clay and a significant component of very fine sand, which locally decreases to (iii_a) <10%; and lastly, (*iv*) a clay-rich unit with >50% content of particles <4 μm in size (Table 1). These classifications are typical of the silt-dominated sediment load of the Ganges and Brahmaputra rivers with variable admixtures of bedload (sand) and washload (clay) material (Datta and Subramanian, 1997).

Five distinct stratigraphic facies (facies A, B, C, D, and E) are also identified (Fig. 4 and Table 2). In each of the stratigraphic sequences, the base is characterized by clean sand (i.e., facies *i*) comprising the shallow aquifer, and

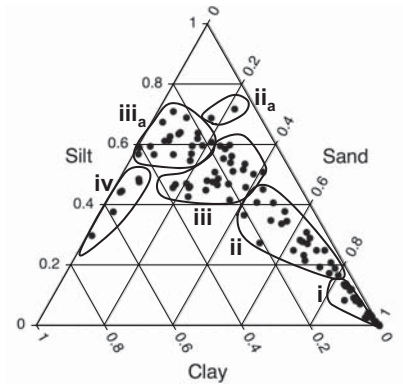

Figure 3. Ternary diagram depicting six sedimentary facies delineated by cluster analysis of median grain size and relative abundance of sands, silts, and clays. Although grain-size distributions reflect a continuum, the facies boundaries shown here were groundtruthed in the field and well reflected associated strata and geomorphic features. Detailed characterization of the sedimentary facies is compiled in Table 1 and discussed in the text.

TABLE 1. SEDIMENTARY FACIES

Sedimentary facies	Lithology	Mean grain size (μm)	Mean sand:silt:clay (% ratio)	Color	Loss-on-ignition (wt%)	Interpreted depositional setting[a]
i	Generally well sorted fine to medium sands	252	90:10:0	Tan to light gray	<1	Channel deposits
ii, ii_a	Silty fine sands to clean silts	73 (ii_a—15)	65:30:5 (ii_a—20:75:5)	Tan to light gray	<2	Bar deposits
iii, iii_a	Poorly sorted, sandy muds to muds	24 (iii_a—12)	25:50:25 (iii_a—10:60:30)	Yellow-brown to brown	2–5	Overbank floodplain deposits
iv	Silty clays	4	10:30:60	Brown to dark gray	5–20	Abandoned channel fill

[a]Sediments have been grouped based on their major environmental association, but the grain-size distributions reveal a continuum of sediment types, and facies are not meant to be exclusive categories.

TABLE 2. STRATIGRAPHIC FACIES

Facies	Stratigraphic sequence	Surface elevation (m)	Thickness of mud cap (m)	Associated sediment facies of mud cap	Distribution in study area	Geomorphic interpretation
A	Generally clean bedded sands near surface, coarsening and becoming massive with depth	8–13	0–0.2	n/a, *ii*	Widespread as curvilinear features (hundreds of meters wide by thousands of meters long); often sites of village settlements	Channel levee or channel bar sequence
B	Alternating sand and mud layers near surface, underlain by clean sands	5–12	Interbedded to 0.5–2 m depth	*ii*, ii_a, *iii*	Relatively local along edges of facies A and transitions to facies C, often cultivated with vegetable crops	Lateral bar sequence
C	Silt-dominated muds with minor interlayers of sand and clay near surface, underlain by clean sands	6–11	0.5–2.5	*iii*, iii_a	Broad, widespread coverage, commonly associated with wheat or rice cultivation (e.g., proximal or distal settings, respectively)	Proximal to distal floodplain sequence
D	Thick, clay-rich muds with minor interlayers of sand and silt, from near surface to depth	6–9	3–9	iii_a, iv_a	Localized in four main areas, often as curvilinear or oblate depressions (tens of meters wide by hundreds of meters long)	Abandoned channel system
E	Variable, but mostly muddy deposits; disturbed and redistributed; underlain by clean sands	8–13	1–5	redistributed *ii*, ii_a, *iii*, *iv*	Widespread in certain villages, particularly those near modern streams or where natural elevations are low and subject to flooding	Anthropogenic fill, usually deposited over levee and bar sequences (facies A and B)

which locally hosts arsenic-bearing groundwater. The thickness and succession of sedimentary facies overlying this basal sand differentiate the five major stratigraphic facies. From generally coarse to fine, the primary sequences include: shallow-aquifer sands that (A) outcrop at the floodplain surface; or are capped by (B) alternating decimeter-scale beds of silt and sand; (C) a variably thick mud unit; (D) a thick (>3 m) clay-rich mud deposit; or (E) highly variable, though generally muddy, anthropogenic fill.

Facies A, where shallow-aquifer sands outcrop or are covered by <20 cm of finer material, is widely distributed as curvilinear or oblate features that are topographically elevated 1–3 m above adjacent floodplains (Table 2). Facies C is similar to A, except that it is bound at the surface by a fine silt, mud, or clay sequence from 0.5 to ~3 m in thickness. Facies C is also widely distributed, occurring throughout the study area as broad, flat plains that are typically used for rice cultivation. In contrast to this broad extent, the alternating sand and silt sequence of facies B is largely restricted to the transition between the higher elevation stratigraphic facies A and lower lying facies C. The alternating beds of fine sand and coarse silt in facies B are ~20–50 cm thick and commonly display cm-scale tabular and trough cross bedding. Facies D is interspersed throughout Araihazar and reflects sites where shallow, fine-grained sediments are several meters thick, locally up to 10 m. Although the surface mud unit in facies D does overlie clean sands, as in the other stratigraphic facies, it is distinguished by its much greater thickness and generally finer grain size (sedimentary facies *iv* and iv_a). The distribution of facies D is restricted but prominent in several low-lying, northeast-southwest–trending depressions that remain wet throughout the year.

Finally, stratigraphic facies E is a common succession within the villages, where the majority of tube wells are located. Facies E is typified by 0.5–3 m of muddy anthropogenic fill that has been placed on top of a previously natural sand stratigraphy (i.e., facies A or B) to provide elevation above flood levels. It appears that the fill most often is composed of the muddy surface unit of facies B and C, which has been dug and transported from the adjacent floodplain. The anthropogenic origin of these units is evidenced by its content of brick, pottery, and garbage, and corroborated by statements from local landowners.

Morphology and Evolution

Geological cross sections constructed by combining sedimentary facies data with digital terrain elevation data (DTED)-derived surface topography illustrate the distribution of stratigraphic units within the floodplain and shallow aquifer (Fig. 5). The cross sections reveal a widespread drape of silts and clays (facies B, C, and D) that overlie shallow aquifer sands, the latter outcropping only in local topographically elevated areas (facies A). This fine mud drape varies in thickness from ~0 to 10 m (facies C and D), with the finest sediments restricted to the upper several meters of floodplain stratigraphy and in the lowest elevation environments (Figs. 2 and 5).

If the mud drape presently covering most of the shallow sand aquifer is not considered, then paleotopography of the former sand surface may be reconstructed (Fig. 2). Such backstripping

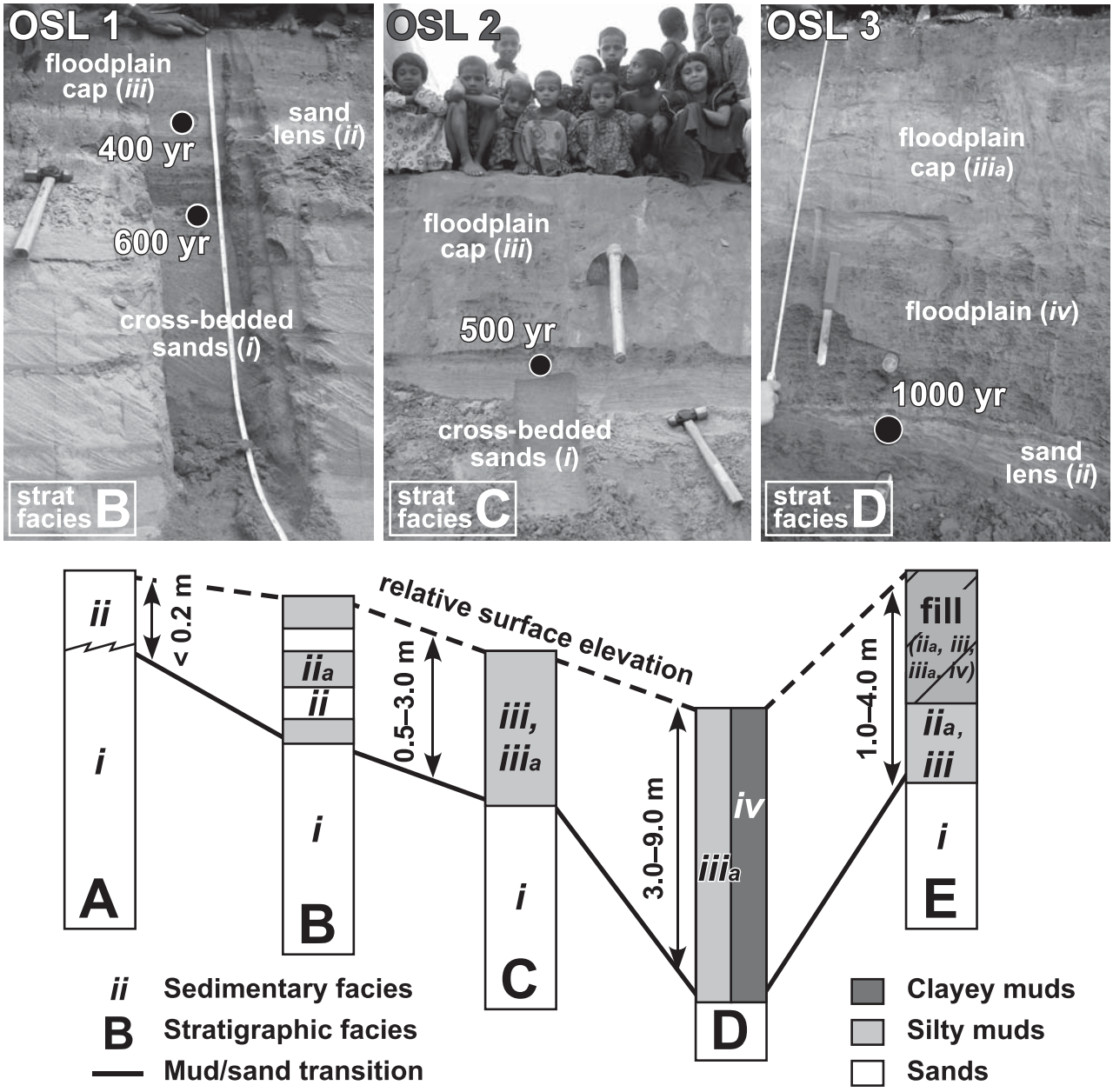

Figure 4. Upper panel—Digital images of the OSL (optically stimulated luminescence) sampling sites and their resulting ages. Site locations are shown in Figure 2. Annotated comments show the distribution of sedimentary and stratigraphic facies, and position of the modern floodplain surface is well indicated by numerous local observers. Note that OSL ages were measured at the boundary from channel sands into floodplain muds, indicating the most recent period of high discharge and active sand transport. Unlike sluggish flow in the modern abandoned channel, decimeter-scale cross bedding reflects dune formation in the previously active braided channel. Lower panel—Generalized stratigraphic facies that represent fluvial subenvironments and sedimentary successions from the study area. A key feature of all successions is that clean sands (i.e., sedimentary facies *i*) underlie all surface units. These sands comprise the shallow aquifer from which groundwater is being extracted by local tube wells. The stratigraphic facies thus distinguished by differing depths to the sand surface (black line) and texture of the overlying floodplain sediments (grayscale). Detailed characterization of the stratigraphic facies is compiled in Table 2 and discussed in the text.

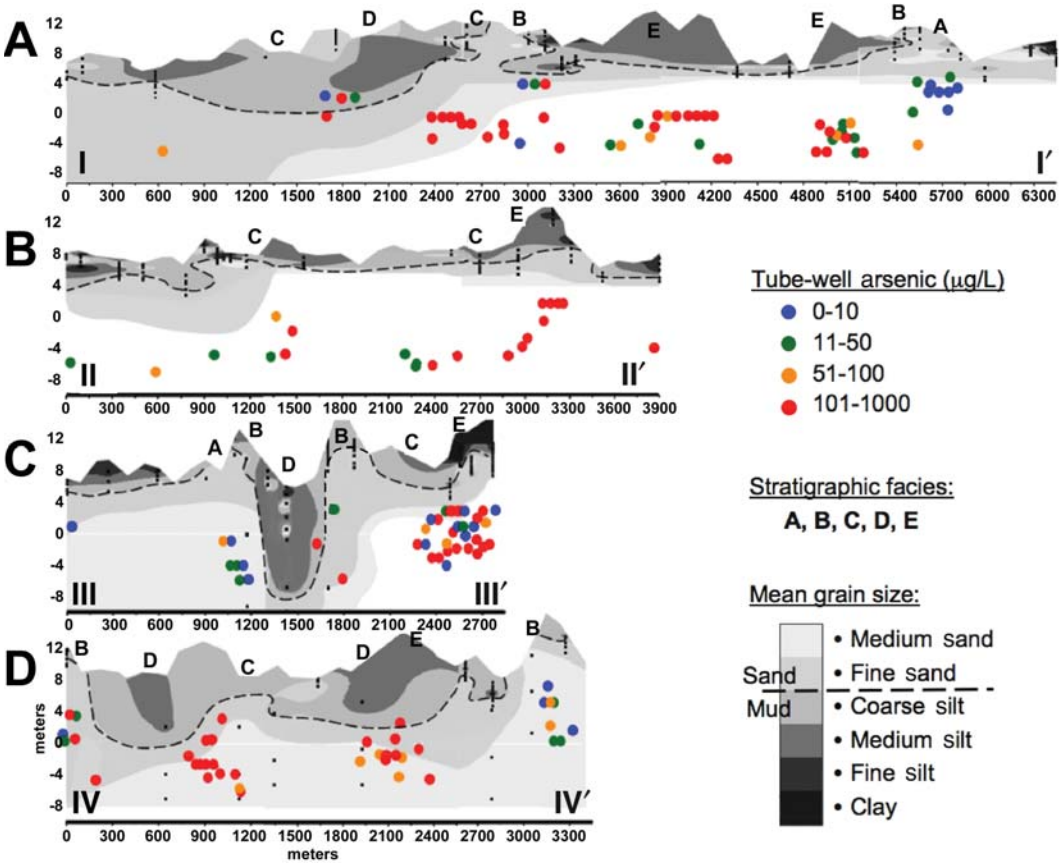

Figure 5. Cross sections showing generalized floodplain stratigraphy, topography, and sediment distribution, superimposed with the depth and arsenic concentration of nearby tube wells. Transect locations (I–I′, II–II′, III–III′, and IV–IV′) are shown in Figure 2. Topographic results were derived from digital terrain elevation data (DTED) (see text). Dissolved arsenic concentrations data are shown for shallow tube wells (van Geen et al., 2003) within 50 m of the transects and plotted at an adjusted depth (DTED elevation minus reported well depth). The observed patterns between floodplain stratigraphy and groundwater arsenic reveal an association of higher arsenic with thicker, finer-grained caps of floodplain sediments, whereas lower concentrations are typically found near outcropping or shallowly buried aquifer sands. A more detailed discussion of these general patterns is given in the text.

reveals sandy deposits of different elevations, which are useful for identifying relict channel, bar, and levee features. The slope of this sand surface between higher and lower elevation features varies from ~0.1° to 9°, with the steeper slopes coinciding with transitions between stratigraphic facies (i.e., facies B). Furthermore, when the paleosand surface is normalized to modern local elevation, the paleotopography of the sand surface is typically preserved. This is especially relevant for villages that have been elevated using anthropogenic fill (facies E), and indicates that these sites were already naturally elevated above the floodplain before being modified by humans (Fig. 5). In areas where topography has been obtained independently from both differential GPS and DTED, each indicates shoaling of the paleosand surface beneath these villages. This similar result between the two data sets demonstrates that clusters of trees within the villages do not dominate our DTED-based observations.

TABLE 3. ACCRETION RATES BASED ON ^{210}Pb AND ^{137}Cs INVENTORIES

Sample	^{210}Pb (dpm/cm^2)	^{137}Cs (dpm/cm^2)	R_{Pb} (cm/yr)	R_{Cs} (cm/yr)
Pb-1A	43	9	0.07	0
Pb-1B	41	16	0.05	0.12
Pb-2A	68	6	0.16	0
Pb-2B	33	8	0.02	0
Pb-3A	64	5	0.14	0
Pb-3B	46	17	0.07	0.15
Pb-4A	10	18	0	0.17
Pb-4B	0	17	0	0.14
Pb-5A	0	5	0	0
Pb-5B	15	0	0	0
Average			0.05	0.06
Standard deviation			0.06	0.08

Note: A and B are duplicate cores from each of the sampling locations.

To determine rates of sedimentation on the modern floodplain, pairs of shallow cores at five sites were analyzed for ^{210}Pb and ^{137}Cs radioisotope geochronology (Table 3 and Fig. 2). The generally low inventories of unsupported ^{210}Pb reflect limited deposition of new sediment within the last century. ^{210}Pb inventories significantly exceeded atmospheric input (25.3 dpm/cm^2; Goodbred and Kuehl, 1998) at only two sites inside the large western meander, accounting for an accumulation rate of ~0.15 cm/yr (Pb-2 and Pb-3; Fig. 2). Overall accretion rates within Araihazar, derived from both ^{210}Pb and ^{137}Cs inventories, are only 0.05 ± 0.06 and 0.06 ± 0.08 cm/yr, respectively. These results agree well with accretion rates recorded from other distal floodplain environments in the Ganges delta (~0.10 cm/yr; Goodbred and Kuehl, 1998) and indicate that the Araihazar floodplains are effectively relict, receiving no significant sediment input within the past century.

Long-term accretion rates derived from the optically stimulated luminescence (OSL) ages of shallow sand layers are also comparable to those determined from ^{210}Pb and ^{137}Cs, with an average rate of 0.12 ± 0.03 cm/yr. Luminescence dating of the paleosand surface at two sites close to the modern stream (OSL 1 and OSL 2; Figs. 2 and 4; Tables 4 and 5) indicates burial of the aquifer sands beginning ~600 years ago. This transition from clean, cross-bedded sands to fine-grained overbank muds indicates decreased fluvial energy and the beginning of abandonment by the main river channel. Sand beds (<15 cm thick) reappear locally within the muddy floodplain cap, and at site OSL 1 yielded an age of ~400 years ago, presumably because of a temporary reactivation or a large flood of the channel around this time. In contrast to these two sites, both of which lie along the large channel feature in the north, the age of the shallowest (i.e., youngest) sand layer at OSL 3 in the meandering scroll plain of northeast Araihazar yields a considerably older age of 1000 years This sand layer is relatively minor (i.e., <5 cm thick

TABLE 4. OPTICALLY STIMULATED LUMINESCENCE (OSL) SUMMARY OF RESULTS

Sample	Depth (cm)	U (ppm)	Th (ppm)	K (%)	No. of aliquots	De (Gy, 10%)	Water (%)	Dose rate (Gy/ka)	Age (ka)	De (wt. mean)	Age (ka)
OSL 1	35	5.9 ± 1.1	11.6 ± 5.9	2.0 ± 0.1	30	1.60 ± 0.04	20 ± 5	3.4 ± 0.4	0.4 ± 0.1	1.9 ± 0.1	0.5 ± 0.1
OSL 1	65	5.5 ± 0.6	24.1 ± 6.7	2.0 ± 0.1	22	2.0 ± 0.1	20 ± 5	4.0 ± 0.5	0.5 ± 0.1	2.7 ± 0.2	0.6 ± 0.1
OSL 2	100	11.6 ± 1.3	15.5 ± 11.3	1.9 ± 0.1	30	3.01 ± 0.03	20 ± 5	4.0 ± 0.7	0.6 ± 0.1	3.7 ± 0.1	0.8 ± 0.1
OSL 3	109	4.9 ± 1.3	9.5 ± 4.5	1.9 ± 0.1	30	3.10 ± 0.08	20 ± 5	3.0 ± 0.5	1.0 ± 0.1	5.0 ± 0.1	1.6 ± 0.2

and mixed with muds) and is at least 1 m shallower than the underlying aquifer sands, implying that the channel formerly occupying this site was abandoned more than 1000 yr ago.

Distributions of Arsenic within the Floodplain

Dissolved arsenic concentrations for 200 shallow wells located within 50 m of the auger transects were identified using a GIS database. The resulting patterns of arsenic distribution are seen to be broadly related to local floodplain geomorphology and shallow stratigraphy (Figs. 2 and 5). In general, the highest arsenic concentrations are associated with thick mud strata (facies D) and both natural (facies C) and anthropogenic (facies E) mud-capped sands. Similarly, areas of lower arsenic concentration are commonly associated with sandy stratigraphy that outcrops or is very shallowly buried (facies A and B, respectively) (Figs. 5A–5D). Aside from these general associations, patterns at the scale of tens of meters show further complexity (see Fig. 5). For example, even within villages with relatively high or low levels of tube-well arsenic, there often are several wells with very different arsenic concentrations. Such anomalies have been suggested to be a result of high vertical, dissolved arsenic gradients (McArthur et al., 2004) or a structural failure and leakage into the tube wells (Cheng et al., 2006). In this paper, however, we focus on the major trends occurring at spatial scales of hundreds of meters because this is the scale over which we sampled and over which floodplain stratigraphy laterally varies.

Transect I–I′

This transect obliquely follows the major, northeast-southwest–trending fluvial system in Araihazar, crosscutting several geomorphic features, including levees, channel bars, and infilled channels (Fig. 2). OSL dates suggest that active fluvial sand deposition persisted in this area until ~600 yr ago, after which the channel and floodplain system was progressively abandoned. Along the eastern end of transect I–I′ (i.e., at a transect distance of 5400–6300 m), sands outcrop (facies A) or are shallowly buried (facies B) in association with relict bar and levee features. Arsenic concentrations in this area are generally low, particularly when compared to middle reaches of the transect. In the middle region, the capping of clay-rich silts thickens in low-lying floodplain and abandoned channel environments (Fig. 5A; facies C and D, respectively). Groundwater arsenic values are generally high in these mud-capped settings, but are seen to decrease even in a relatively narrow region where sands locally reach the surface (e.g., ~3000 m). Notably, humans have emplaced much of the thick, surficial mud cap found at 3600–4200 m and 4800–5100 m to raise the village elevation above high floodwaters. As illustrated here, this modified stratigraphy (facies E) is commonly associated with high levels of arsenic in shallow groundwater.

Transect II–II′

This transect (Fig. 5B) traces a morphology similar to that of transect I–I′, but in the northeast it crosscuts the more meandering channel system that is over 1000 yr old (~3400–3600 m). Again, enrichments in shallow groundwater arsenic correspond to sections of thicker mud-capped sands, notably in the village at ~3000–3300 m that has been artificially capped with muds (facies E).

Transect III–III′

This transect, perpendicular to I–I′ and II–II′, reveals broadly similar patterns (Fig. 5C), with high dissolved arsenic below the anthropogenically filled village area (~2700 m) and low arsenic concentrations below unmodified, sand-dominated stratigraphy (facies A, ~1200 m). However, transect III–III′ encompasses some of the most contrasting sediment lithologies in Araihazar, of both natural and anthropogenic origin, that occur over short distances. In terms of natural stratigraphy, one of the thickest examples of muddy channel fill (facies D; ~1500 m) is juxtaposed with >3 m of alternating layers of sands and muds (facies B; ~1800 m) more than 6 m higher in elevation. Tube-well arsenic values in this area (at ~1800 m) are very high (>100 µg/L), with local-scale processes (10^1 m) presumably playing an important role where floodplain stratigraphy is so strongly heterogeneous. An example of heterogeneous stratigraphy associated with anthropogenic activity is found in the village at 2400–2700 m (facies E). The site is capped by some of the finest grained sediments (facies iv_a) in Araihazar, although field observations indicate that they are patchily distributed (this patchiness is not expressed in Fig. 5C due to the large scale). Again, the spatial heterogeneity of the stratigraphy appears to be reflected in shallow-aquifer arsenic concentrations, with a mixture of clean and contaminated wells found between 2400 and 2700 m.

TABLE 5. ACCRETION RATES BASED ON OPTICALLY STIMULATED LUMINESCENCE (OSL) DATA

OSL site	cm	yr	cm/yr
1	35	400	0.09
1	65	600	0.11
1-middle	30	200	0.15
2	100	500	0.20
3	109	1000	0.11
Average			0.13
Standard deviation			0.04

Transect IV–IV′

This transect also crosses the older meandering channel system in northeast Araihazar and is characterized by a largely continuous and natural cap of floodplain deposits and fine-grained channel fill. High groundwater arsenic in the shallow aquifer is once again seen to be concentrated below thick, fine-grained strata between 300 and 2700 m. In immediately adjacent areas (~100 and 3300 m), arsenic concentrations drop considerably in conjunction with a more sand-dominated shallow stratigraphy (facies A and B), providing a notable contrast.

Regression Analysis

The qualitative linkages between arsenic and stratigraphy described above were more quantitatively evaluated by plotting arsenic concentration as a function of minimum, mean, and maximum depth-to-sand using the zonal statistics spatial analyst function of ArcView 8.3 (Fig. 6). The depth-to-sand values were taken from the paleosand-surface interpolation in Figure 2, and for each well, the program overlies the two data sets to return the minimum, mean, and maximum depth-to-sand values for each value of arsenic in tube wells between 6 and 15 m deep. Since the auger and needle sampling locations are spatially limited, results of the comparison are not, at this point, predictive. The results, however,

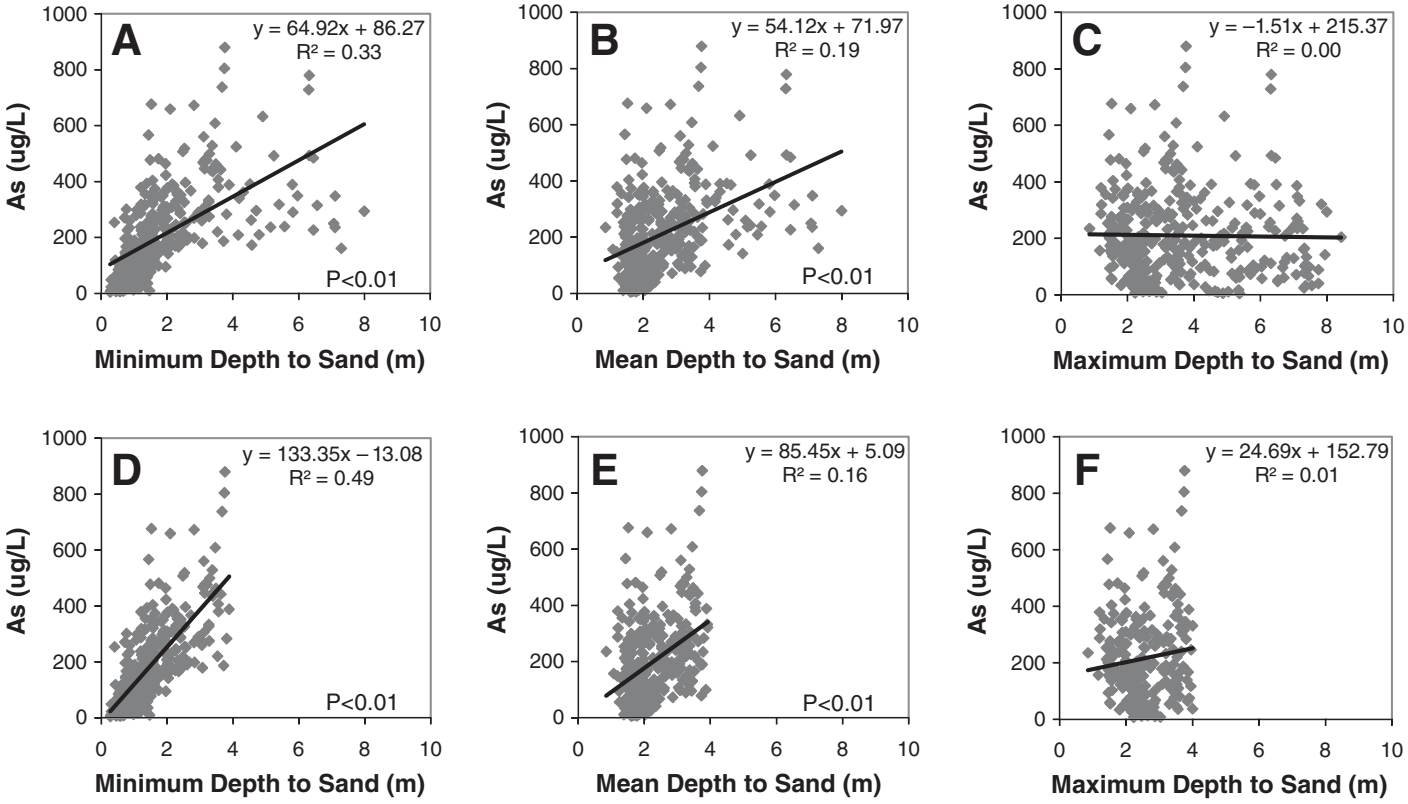

Figure 6. Correlation plots for depth-to-sand values and shallow (<23 m) tube-well arsenic concentrations. The depth-to-sand measurements are plotted as minimum, mean, and maximum values as determined from the interpolation shown in Figure 2. The upper plots (A, B, and C) include all values, whereas the lower plots (D, E, and F) exclude depth-to-sand values >4 m. These values are excluded because it is rare for a tube well to be installed beneath the thickest muds, and thus the corresponding arsenic value is more likely from a tube well just adjacent to these muds (such patterns are seen in Fig. 5). This would also explain the weakest correlation for maximum depth-to-sand values, compared with results for minimum and mean values. In contrast, the correlation of minimum depth-to-sand with arsenic shows considerable explanation of variance (R^2 = 0.33 and 0.49 at p <0.01) and appears to most accurately reflect the linkage of floodplain cap thickness and tube-well arsenic. Overall these results support a moderate but statistically significant correlation between arsenic and depth-to-sand.

do display the general trend of increasing arsenic with increasing thickness of the mud layer, which is what was observed in the field and in our stratigraphic transects. Though relatively weak (R^2 = 0.33–0.49), the correlations between arsenic concentrations and minimum depth-to-sand values are significant (p <0.01) and support our qualitative findings (Figs. 6A and 6D). The relationship weakens slightly when mean depth-to-sand is considered instead (Figs. 6B and 6E), and effectively disappears when considering maximum depth-to-sand (Figs. 6C and 6F). This is probably because areas with thicker mud units are less likely to be tapped for tube wells, although there may be other reasons. The better fit with minimum depth-to-sand values likely indicates that arsenic concentrations are more closely linked with a tube well's proximity to shallow or outcropping sands as opposed to the thickness of a particular mud sequence.

DISCUSSION

Correlation of Fluvial Geomorphology with Patterns of Shallow Groundwater Arsenic

Although the thickness and distribution of near-surface muds are shown to be heterogeneous (Figs. 2 and 5), these patterns are not random and can largely be defined within traditional fluvial geomorphic classifications. A geomorphic reconstruction of the Araihazar area (Fig. 7) integrates data from more than 100 hand-drilled augers and needle samples, over 75 km of electromagnetic (EM) conductivity coverage (van Geen et al., 2006a), luminescence dating, and planform analysis of satellite images. The resulting patterns delineate features of a formerly large, braided river system, including bars, levees, and infilled channels. The braided-channel system is also seen to crosscut the meander bends of at least two older, more sinuous fluvial systems, each of which consists of a complex of lower-lying levees, infilled channels, and scroll bars (Fig. 7). Both braided and meandering river planforms are common in Bangladesh (Rasid, 1966; Coleman, 1969).

The distribution of tube wells (i.e., the sites of homes and villages) in this complex setting is not, surprisingly, aligned with elevated geomorphic features, such as bars and levees, where seasonal flooding is less frequent. This relationship can be seen when groundwater arsenic concentrations are overlain onto a map of geomorphic features (Fig. 7). Tube wells that are associated with individual geomorphic features generally support either high or low arsenic values, or at least large clusters of similarly contaminated wells. In this paper, we focus on these general trends in the more predictable and

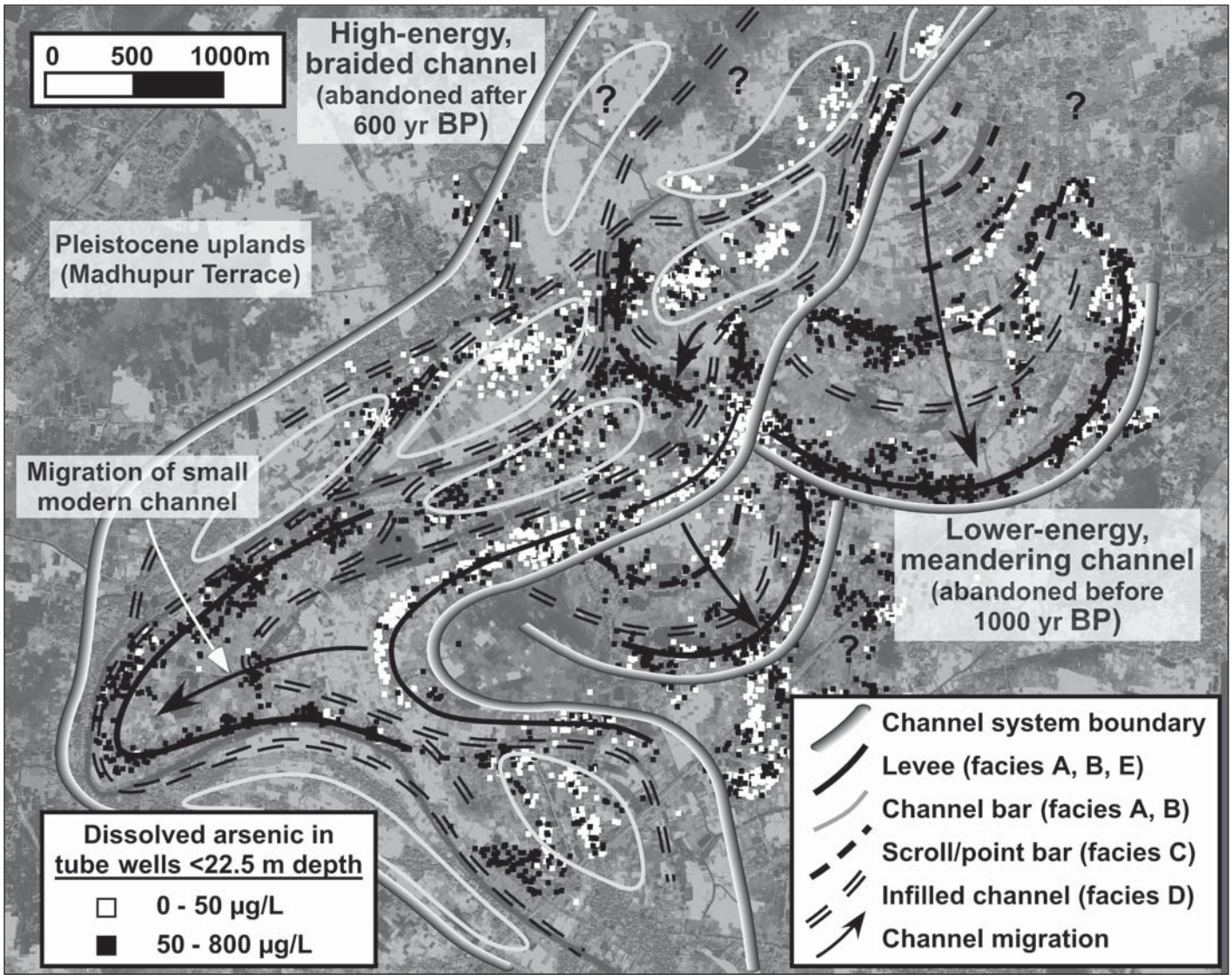

Figure 7. Geomorphic map of surface and shallow landforms in Araihazar, shown with shallow tube wells of high- and low-arsenic concentrations. The geomorphic features were identified using land surface and depth-to-sand topography in conjunction with sedimentary and stratigraphic facies recorded during hand augering. Ages of the channels are constrained by optically stimulated luminescence (OSL) dates. Results reveal the now-abandoned features of a younger, multi-thread braided channel that crosscuts two older, single-channel meander bends. The braided stream is characterized by large, sandy channel bars and generally higher relief and overall elevation than the meandering point-bar sequences. The location of tube wells (i.e., homes and villages) is typically found on higher elevation features such as levees and bars. However, those features formed by lower energy meandering streams or near mud-filled channels are associated with thicker, finer-grained surface sediments and generally high groundwater arsenic.

definable context of floodplain evolution and geomorphology.

Channel Bars

Perhaps the best defined association of arsenic with geomorphic features is the consistently low arsenic values that occur on channel bars within the former braided channel system (Fig. 7). These areas typically comprise stratigraphic facies A and B, with aquifer sands lying at or near the surface. The reason for their relatively high elevation and sandy stratigraphy is that the bars developed during seasonally high river stage and flow regime (Bridge, 1993). This occurs during the summer monsoon when discharge is approximately ten times greater than the dry season (Coleman, 1969). Luminescence ages indicate that progressive abandonment of this high-energy braided channel began after 600 years ago. This probably continued until about one hundred years ago when the main Brahmaputra finally avulsed to its modern course far from Araihazar (Fergusson, 1863). The waning of discharge associated with abandonment would have led to a comparative decrease in seasonal flood height and flow velocity (Bristow, 1999). Such lower flow regimes would have favored the widespread capping (facies C) and infilling (facies D) of the sandy, braided-channel topography with fine-grained sediments. Locally elevated areas, such as the channel bars, would infrequently flood and thus leave sand still exposed at or near the floodplain

surface. Consequently, villages became settled on these sandy elevated areas and today yield shallow groundwaters relatively low in arsenic compared with adjacent, muddier areas.

Levees

River levees are also common sites for human settlement, as can be seen by the elongate, curvilinear arrangement of tube wells in many areas (Figs. 2 and 7). Again, this settlement pattern arises partly because of the levees' relatively high elevation and due to their proximity to water channels for transportation. However, in contrast with the relative homogeneity of tube-well arsenic on the channel bars, arsenic in wells associated with the levees differs considerably between the individual features. For example, some levees support almost exclusively contaminated wells, whereas others yield mostly clean, shallow groundwater (Fig. 7). Consistent with our observations, the main sedimentological difference in levees with high or low groundwater arsenic is the thickness and extent of the surface mud cap. In low-arsenic levees, shallow aquifer sands lie exposed at or near the floodplain surface (facies A); levees with contaminated groundwaters are almost exclusively those with thick mud caps (facies C and E).

What, then, is the geomorphic difference between these two types of levees? It appears that the more contaminated, mud-capped levees are largely found along the older, meandering scroll plain region in northeast Araihazar, reflecting development in a relatively low-energy fluvial regime. In contrast, the sandier, less contaminated levees are located mainly in the former braided-channel region and consequently developed under higher energy flow regimes. The most prominent, low-arsenic levee is that which forms the southern boundary of the former braided stream channel. More contaminated levees are associated with the laterally migrating meanders of a sinuous stream (as indicated by the black arrows; Fig. 7). Because these levees were formed under a lower energy regime, they are consequently finer grained and lower elevation.

The latter point gives rise to another major factor that we believe may locally exacerbate arsenic contamination. Apparently because many levees, particularly those lower in elevation, flood with some frequency, many have been anthropogenically modified by filling the surface with fine-grained sediment to increase elevation (facies E). This artificial capping of levee environments was repeatedly observed during fieldwork by the presence of anthropogenic debris in surficial deposits. The modifications can also be recognized from our shallow geologic cross sections (e.g., Fig. 5B, 3150 m; Fig. 5C, 2700 m). Thus, we find that human modification of the floodplain may act as a significant "geological" agent that leads to a mud-capped stratigraphy mimicking the natural conditions associated with high arsenic levels in shallow groundwater of Araihazar.

Scroll Bars

Scroll bars are low-lying, sandy ridges formed along the inner edges of river meanders. The scrolls actually originate as the point bars of an active meander loop, but ultimately evolve into a plain of scroll bars as the meander migrates laterally toward its outer edge and abandons the active point bar (Hickin, 1974). Several sandy scroll-bar complexes are found in Araihazar along the inner edges of the older meandering channels (Fig. 7). The natural scroll bar features in Araihazar appear to be relatively low lying, perhaps only 1–2 m above the adjacent floodplain. However, in many circumstances, the scrolls appear to have been modified with anthropogenic fill, thereby increasing their elevation and thickness of the mud cap (e.g., 3250 m, Fig. 5B). The general distribution pattern of groundwater arsenic along the scroll bars is similar to that of the levees, where certain clusters of wells (over hundreds of meters) are either largely clean or largely contaminated.

Floodplain Evolution

The progressive impact of different fluvial regimes on the morphology of Araihazar, and therefore on the arsenic content of shallow groundwater, can be summarized schematically (Fig. 8). The initial stage considers a large, active, braided river system, similar to that of the modern Brahmaputra, which is kilometers wide with multiple channels and bars (Coleman, 1969). Bristow (1987) describes how migration of the braided Brahmaputra channel planates the preexisting floodplain surface, replacing eroded sediments with almost exclusively channel sands and sandy bar deposits. Based on close proximity of the paleo-Brahmaputra channel before 200 yr ago, we infer that the largely contiguous shallow-aquifer sands of present-day Araihazar were deposited in a similar manner. Ultimately, river avulsion is initiated and results in progressive abandonment of this braided channel, which may take place over many decades (Fergusson, 1863). Because avulsion often occurs over long time periods in the Bengal basin, the river planform actually adjusts to declining flow by switching from a braided to a meandering system (Bristow, 1999). Based upon the depositional ages of sediments, we know that this abandonment began after 600 yr ago. With waning flow conditions, the large channels and interbar depressions begin infilling with fine-grained sediment. This process continues until most of the topography is infilled or the area no longer receives sediment (cf. Rasid, 1966). The negligible accretion rates measured in Araihazar (Table 3), as well as its relatively flat topography and lack of large modern channels, suggest that most of the area infilled prior to complete abandonment. We presume that fine-grained sediment accretion was relatively rapid (>0.20 cm/yr) until about one hundred years ago when the main course of the Brahmaputra switched to its present course west of the Madhupur Terrace (Fergusson, 1863). This final "moribund" stage would be appropriate for human settlement with exposed, sandy, high grounds as village sites and muddy floodplains for agriculture. Indeed, residents of Araihazar report that a "big" river occupied the area until at least one hundred years ago.

Possible Mechanisms for Shallow Geological Controls on Groundwater Arsenic

What might be some of the plausible controls of floodplain stratigraphy on arsenic concentrations? One reason for the different arsenic-bearing capacities between these villages can be attributed to the ways in which sediment grain size impacts chemical and physical processes that control arsenic reaction and transport within the aquifer. The main feature of the integrated set of our observations is that peaks in shallow groundwater arsenic correspond to areas overlain by, or sometimes near to (i.e., on the order of tens of meters), thick surficial deposits of silt and clay. Locations where arsenic levels diminish are typically characterized by coarser sediments proximal to the ground surface. We therefore suggest that such surface to near-surface exposures of shallow-aquifer sand locally enhance the flushing rates of the aquifer. Such a connection has recently been substantiated by tritium-helium dating of groundwater within the Araihazar study area (Stute et al., 2007). The fact that these recharge-capable sands occur in typically elevated portions of the floodplain—as in the case of natural levees and bars—is not insignificant, since the additional elevation can set up a higher hydraulic head (Fig. 9). Even in the absence of significant recharge, the greater potentiometric surface of the elevated sands limits flow into these areas from the low-lying, fine-grained settings that frequently have higher levels of dissolved arsenic.

By the same token, finer sediments could potentially enhance arsenic mobilization by increasing groundwater residence time (Stute et al., 2007). Hydrologically, this can be attributed to the reduction in hydraulic conductivity associated with decreasing grain size. An order-of-magnitude comparison of floodplain transmissivity

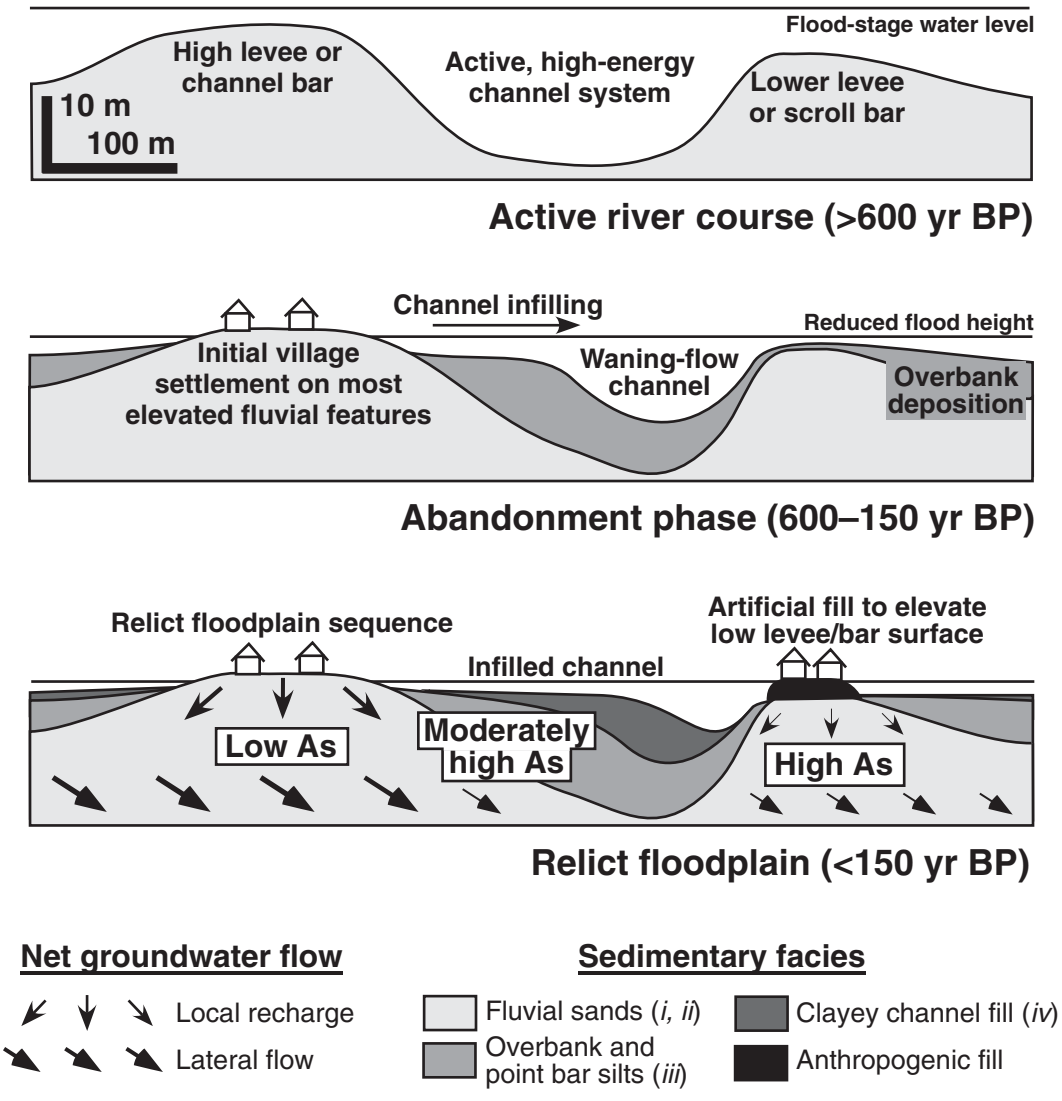

Figure 8. Generalized model of floodplain evolution and aquifer development in Araihazar, here suggested to be a first-order control on the heterogeneity of shallow groundwater arsenic. The first stage portrays the region before 600 years ago, when the Brahmaputra river flowed east of the Madhupur Terrace either through or near to Araihazar. Similar to the modern Brahmaputra braidbelt, thick channel and bar sands were deposited, which today comprise the shallow aquifer. The second stage reflects progressive channel abandonment beginning after 600 years ago, when the main channel shifted to its penultimate course north of Araihazar. This period is characterized by channel infilling and overbank deposition of fine-grained sediments. The final stage begins after 150 years ago, when the Brahmaputra avulsed to its modern course, thereby further reducing sedimentation rates and leaving the largely moribund, muddy floodplain of today.

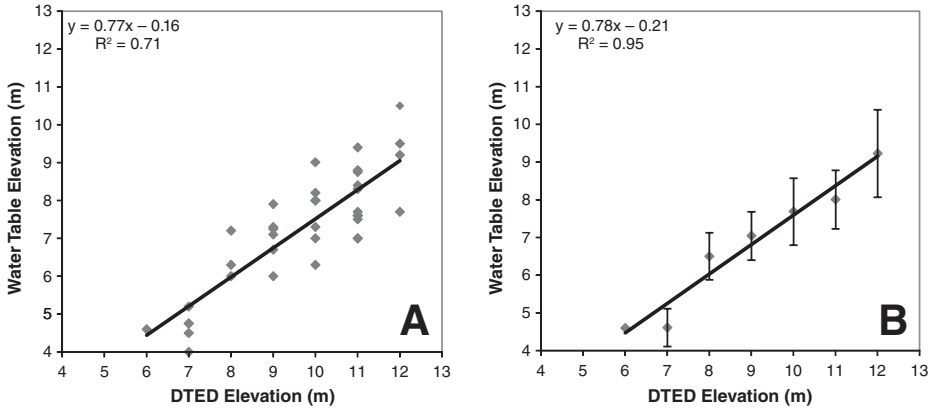

Figure 9. Correlation plots for surface topography and water table elevation in Araihazar. (A) Graph of data for all water table measurements and (B) a regression using only the average water-table elevation for a particular topographic elevation. Depth to the water table is relative to the digital terrain elevation data (DTED) and is recorded for 36 augers during field sampling in January 2003. Sampling elevations between ~6–9 m were taken in the low-lying floodplain cultivated by the farmers from adjacent, more elevated villages (>10 m).

can be made using the Hazen approximation, $K = C(d_{10})^2$, whereby the hydraulic conductivity of the sediment K (m/s) is equal to a proportionality coefficient C (65) multiplied by the effective particle diameter such that 10% of the distribution is finer than the square of this diameter (d_{10}). An equivalent vertical conductivity for the upper 15 m of sediment can be calculated using the harmonic mean of the samples, $K_z = 15/(\Sigma_i^n b_i/K_i)$, where b_i and K_i are the thickness (m) and conductivity (m/s) of the sublayer, respectively (Ingebritsen and Sanford, 1998). The resulting range of vertical groundwater conductivities, from millimeters to meters per day (~10^{-5} to 10^{-9} m/s), is comparable to the typical K value calculated for the silty floodplains in the region of Araihazar (4.6×10^{-6} m/s; BGS/DPHE, 2001). If these values are considered in the absence of horizontal flow, and assuming a vertical gradient close to unity, then the corresponding transport time of groundwater to a depth of 15 m would range from 17 days to 47 yr, which is comparable to actual measurements determined by $^3H/^3He$ (Stute et al., 2007). If groundwater flow is indeed controlled by sediment grain size and floodplain architecture, then the heterogeneous stratigraphy observed here could be a salient characteristic of groundwater movements at the scale of 10^1–10^2 meters, typical of village structure and tube-well distributions.

While such an exercise oversimplifies aquifer flow, it does show how general facies distribution can aid in predicting groundwater ages in Araihazar. If a vertical gradient on the order of 10^{-4} is considered (Martin Stute, 2006, personal commun.), time scales of 10^3 to 10^7 years would be required for water to reach a depth of 15 m. Since groundwaters at this depth are known to be younger, ~1–30 yr, in Araihazar (Stute et al., 2007), then either the vertical gradient is greater than those measured (>10^{-4}) and thus recharge occurs more rapidly, or a portion of young water is being advected horizontally. An estimate of horizontal conductivity [$K_x = (\Sigma_i^n K_i b_i)/15$] indicates values 10^{-5} to 10^{-8} (m/s) and horizontal gradients are from 10^{-3} to 10^{-5} (Martin Stute, 2006, personal commun.), which suggests that the farthest distance the young groundwater observed in Araihazar could have flowed horizontally is less than 100 m. This model constraint, in conjunction with the apparent absence of horizontal mixing of arsenic observed in the stratigraphic cross sections (Fig. 5), strongly suggests that horizontal flow does not dominate the age or distribution of arsenic in Araihazar's shallow groundwater. This is presumably why juxtaposing villages and wells can have such differences in shallow groundwater arsenic; it is due to localized flow patterns constrained by the shallow stratigraphy.

The apparent significance of stratigraphically mediated groundwater flow is further enhanced by the observation that an easily mobilized fraction of arsenic exists on the shallow Holocene sands of Araihazar (Zheng et al., 2005). In this case, rapid release of arsenic into groundwaters of locally variable flow rates would have a direct impact on dissolved arsenic concentrations and may explain why arsenic appears well correlated with surface sediments and shallow stratigraphy. This idea differs from previous speculations where higher vertical flow is thought to increase arsenic concentrations by advecting arsenic and/or groundwater reductants to depth (BGS/DPHE, 2001; Harvey et al., 2002). Instead, our findings suggest that vertical flow gradients can be greater than the 1:10 horizontal to vertical ratio commonly assumed by these studies (BGS/DPHE, 2001), especially where aquifer sands reach the floodplain surface, and thus may be sufficient to locally prevent arsenic from accumulating in the groundwater. In contrast, areas overlain by thick, fine-grained sediments likely experience less of a vertical gradient, hence limited recharge and flushing of arsenic (cf. Stute et al., 2007).

Redox state and presence of an easily mobilized arsenic phase are also likely important controls on shallow aquifer arsenic. For example, rapid recharge by oxic groundwater can affect arsenic speciation and favor iron-oxyhydroxide stability, thereby attenuating dissolved arsenic concentrations (Suiling and Mulligan, 2006). Alternatively, in abandoned channels with thick, fine-grained sediment sequences, recharge is slow and can enable the local aquifer to become more reducing and more prone to arsenic mobilization (Fig. 8; Nickson et al., 2000). It is therefore likely that local arsenic heterogeneity is due to a combination of recharge and aquifer redox states, both of which vary in response to the grain size and shallow stratigraphy of the floodplains in Araihazar. Recent high-resolution needle-sampling of groundwaters supports this hypothesis, since simultaneously sampled water and sediments in Araihazar show low dissolved arsenic concentrations coinciding with more permeable layers (van Geen et al., 2006c). Additional findings of the suppressed release of arsenic under oxic conditions (Radloff et al., 2007) indicate that redox plays a key role in its dissolution.

CONCLUSIONS

In the absence of successful hydrological modeling of arsenic over local, 10–1000 m spatial scales, the geomorphic approach could represent a plausible approach for understanding arsenic distributions. In one of the first efforts to explain heterogeneity at this more relevant, human scale, we demonstrate that geology can explain much of the local heterogeneity of arsenic in the shallow aquifer of Araihazar, Bangladesh. Results show that surface depositional features formed under high-energy, braided-channel conditions, including levees and bars, typically have the highest natural elevation and comprise permeable sands from the ground surface to depths typical of the shallow aquifer (15–25 m). Such environments are those most commonly associated with low arsenic concentrations in groundwater extracted from tube wells. Other levee features formed under the lower energy conditions of a meandering system are lower in elevation and comprise finer sediments in the upper few meters of stratigraphy. Tube wells located on meandering stream levees are typically associated with higher groundwater arsenic, which is evidently linked with a thicker and finer grained floodplain cap. The relatively weak but statistically significant relationship (R^2 = 0.33, $p < 0.01$) between arsenic and near-surface geology and geomorphology indicates a level of predictability that is relevant at the village scale. The apparent relationship between human modification of the floodplain and high arsenic levels warrants further investigation. Whereas no direct relationship is established here, anthropogenic activities around village tube wells can be extensive and result in meters of fine-grained fill capping the natural stratigraphy. Such areas typically support high concentrations of arsenic and mimic the type of floodplain stratigraphy associated with high groundwater arsenic.

APPENDIX: METHOD DESCRIPTIONS

Sediment Grain Size and Facies

Sediment samples were collected along four primary transects across the study area (I–I′, II–II′, III–III′, and IV–IV′), with augering sites nested to capture both larger scale (10^3 m) and smaller scale (10^1–10^2 m) variability in the distribution of shallow groundwater arsenic (Fig. 2). Of the 95 hand augers, 56 were located in low-lying cultivated fields where deposits are relatively undisturbed, as compared with many village areas where there has been significant anthropogenic reworking and addition of sediment. Of the remaining auger samples, 11 were from eight villages with drastically different tube-well arsenic concentrations (village means ranging from 5 to >500 µg/L), and 28 augers were collected next to shallow tube wells (<15.2 m) with dissolved arsenic concentrations ranging from 5 to 879 µg/L. All augers were drilled through the surface mud cap and typically 50 cm or more into the underlying

sand unit (i.e., the shallow aquifer, up to ~6 m). Sediment samples from 6 to 23 m depth were acquired using the local hand drilling technique modified for needle sampling (van Geen et al., 2004).

The characterization and interpretation of stratigraphic facies were based on detailed field descriptions and validated by grain-size analysis of a subset of 129 samples taken from 19 auger and 11 needle-sampling locations. Grain-size distributions were determined using a settling tube for sediment fractions greater than 63 μm and a Micromeritics Sedigraph 5100 for the <63 μm fraction (Lamy et al., 1998). The organic fraction associated with each sample was determined by loss-on-ignition (LOI) at 450 °C for 6 h. A cluster analysis of the measured LOI, sand (>63 μm), silt (4–63 μm), and clay (<4 μm) fractions using unweighted pair-group averaging and Euclidean distancing of the variables was performed to identify major sedimentary facies in the floodplain (Clifford and Stephenson, 1975). Clustering results were consistent with field descriptions and sedimentary facies previously identified in the Bengal basin (Ahmed et al., 2004; Goodbred and Kuehl, 2000).

Sediment Accretion and Dating

Sediment accretion rates were determined using ^{137}Cs and ^{210}Pb radionuclide inventories (He and Walling, 1996; Goodbred and Kuehl, 1998) measured along a transect of ~1 km from a point bar along the modern channel to the distal floodplain (Fig. 2). Samples of fine-grained surface sediments were collected using a 50-cm push core (n = 10), separated into two 25-cm intervals, which were then dried, homogenized, and weighed into ~100 g portions into sealed containers. The activity of ^{137}Cs ($T_{1/2}$ = 30.17 yr) and ^{210}Pb ($T_{1/2}$ = 22.3 yr) was determined by gamma spectroscopy using a low-energy (planar), intrinsic germanium detector. Each sample was allowed to reach secular equilibrium with parent ^{226}Ra ($T_{1/2} = 1.60 \times 10^3$ yr) and corrected for self-absorption of the low-energy ^{210}Pb gamma emission (Cutshall et al., 1983). On the basis of ^{137}Cs and ^{210}Pb inventories at each site, floodplain sedimentation rates were calculated using the method described by He and Walling (1996) and Goodbred and Kuehl (1998). Minor discrepancies between ^{137}Cs- and ^{210}Pb-derived accretion rates are not unexpected given the different input histories for these nuclides as well as the complexity of floodplain sedimentation patterns (He and Walling, 1996; Aalto et al., 2003).

Aquifer sands were dated by optically stimulated luminescence (OSL), which measures the amount of time since a unit of sediment has been exposed to sunlight (i.e., the time lapsed since burial) (Jain et al., 1999; Kale et al., 2000; Srivastava et al., 2001). Samples were taken at three locations (OSL 1, OSL 2, and OSL 3; Fig. 2), either from sandy deposits directly underlying the fine-grained floodplain cap (depths 65, 100, and 109 cm) or sand layers within the muddy floodplain cap (depth 35 cm). In total, four samples were retrieved, two of which were from successive layers (OSL 1). The dates of the samples give times that high-energy fluvial processes were active at each of the locations.

For OSL dating of the Araihazar samples, quartz grains were extracted after a sequential treatment with 1N HCl and 30% H_2O_2 to remove carbonate and organic matter, respectively. Following mineral separation using sodium polytungstate (2.58 g/cc), quartz-rich grains of 90–125 μm size were selected by sieving and etched for 80 min in 40% HF. Luminescence measurements were made using blue light stimulated luminescence (BLSL; 470 nm, ~50 mW/cm^2) through a U-340 and Schott BG-39 filter combination on an upgraded thermoluminescence (TL)/OSL Riso TL-DA-15 automated system. External dose rate was measured using thick source ZnS (Ag) alpha counting, and gamma counting was used for potassium determination. Equilibrium in the decay chains was assumed, and the cosmic-dose-rate estimation was based on Prescott and Hutton (1988). Paleodoses were determined on 20–30 aliquots by single-aliquot regeneration (SAR protocol; Murray and Wintle, 2000). Results from individual aliquots were rejected if there was a poor fit of the growth curve or if the recycling ratio fell beyond the range 1.0 ± 0.1. Age computations were based on a weighted mean of the minimum 10% of paleodoses with a weighted mean of all the paleodoses calculated for comparison. Experimental errors may include those in paleodose measurements (photon statistics), measurement of K, U, Th, and in source standards and calibrations.

Paleotopography and Modern Floodplain Elevations

A coarse, paleosurface map of Araihazar was constructed from the auger data by interpolating field measurements of depth-to-sand measurements on a 25 m × 25 m cell-sized raster using the spatial analyst in ArcViewGIS. The resulting paleosurface was then projected over IRS-1D Panchromatic and Ikonos imagery (Fig. 2). This paleosand surface was not corrected relative to the modern elevation difference in Araihazar due to the limited number of auger locations.

Modern floodplain elevation data were used to vertically reference the four coring transects (I–I′, II–II′, III–III′, and IV–IV′; Fig. 2) and reconstruct cross-sectional stratigraphies. The relative vertical position of stratigraphic facies was adjusted according to Shuttle Radar Topography Mission (SRTM) digital terrain elevation data (DTED) and interpolated into cross-sectional profiles for paleotopographic interpretation. The SRTM DTED Level 1 data comprise elevations at 90-m post spacings, a suitable resolution for distinguishing differences in geomorphology over spatial scales of 100–1000 m.

ACKNOWLEDGMENTS

The authors would like to thank Uttam Karmaker, Ashraf Seddique, and Mohammed Hoque from the University of Dhaka's Geology Department and Penny Youngs from Stony Brook University's Marine Sciences Research Center for their help in the field. We would also like to thank Stony Brook University's Bob Aller and Teng-fong Wong, Lamont Doherty's Allan Horneman, Martin Stute, and Zhongqi Cheng, along with anonymous reviewers for their help, insight, and comments on the work presented in this paper. Chris Small and John M. Sharp Jr., University of Texas, helped digitally and schematically map the floodplain. We also would like to acknowledge David Amiel and David Hirschberg for help with radiometric analyses. Columbia University's work in Araihazar is supported by National Institute of Environmental Health Sciences (NIEHS) Superfund Basic Research Program grant NIH 1 P42 ES10349 and National Science Foundation (NSF) grant EAR-0345688. Funding for this work was also provided by NSF awards EAR-0229600 and EAR-0345777 to Goodbred. This paper is presented under the United Nations Educational, Scientific and Cultural Organization-International Union of Geological Sciences (UNESCO-IUGS)–supported project IGCP-#475 Deltas in the Monsoon Asia-Pacific Region: DeltaMAP.

REFERENCES CITED

Aalto, R., Maurice-Bourgoin, L., Dunne, T., Montgomery, D.R., Nittrouer, C.A., and Guyot, J.L., 2003, Episodic sediment accumulation on Amazonian flood plains influenced by El Niño/Southern Oscillation: Nature, v. 425, p. 493–497, doi: 10.1038/nature02002.

Acharyya, S.K., Lahiri, S., Raymahashay, B.C., and Bhowmik, A., 2000, Arsenic toxicity of groundwater in parts of the Bengal basin in India and Bangladesh: The role of Quaternary stratigraphy and Holocene sea-level fluctuation: Environmental Geology, v. 39, no. 10, p. 1127–1137, doi: 10.1007/s002540000107.

Ahmed, K.M., Bhattacharya, P., Hasan, M.A., Akhter, S.H., Mahbub Alam, S.M., Hossain Bhuyian, M.A., Imam, M.B., Khan, A.A., and Sracek, O., 2004, Arsenic enrichment in groundwater of the alluvial aquifers in Bangladesh: An overview: Applied Geochemistry, v. 19, p. 181–200, doi: 10.1016/j.apgeochem.2003.09.006.

Berg, M., Tran, H.C., Nguyen, T.C., Pham, H.V., Schertenleib, R., and Giger, W., 2001, Arsenic contamination of ground and drinking water in Vietnam: A human health threat: Environmental Science and Technology, v. 35, p. 2621–2626, doi: 10.1021/es010027y.

Bibi, M.H.F.A., and Ishiga, H., 2006, Distribution of arsenic and other trace elements in the Holocene sediments of the Meghna River Delta, Bangladesh: Environmental Geology, v. 50, no. 8, p. 1243–1253, doi: 10.1007/s00254-006-0298-x.

Bridge, J.S., 1993, The interaction between channel geometry, water flow, sediment transport, and deposition in braided rivers, *in* Best, J.L., and Bristow, C.S., eds., Braided

rivers: Geological Society of London Special Publication 75, p. 13–71.
Bristow, C.S., 1987, Brahmaputra River: Channel migration and deposition, *in* Etheridge, F.G., Flores, R.M., and Harvey, M.D., eds., Recent developments in fluvial sedimentology: Tulsa, SEPM (Society for Sedimentary Geology), p. 63–74.
Bristow, C.S., 1999, Gradual avulsion, river metamorphosis and reworking by underfit streams: A modern example from the Brahmaputra River in Bangladesh and possible ancient example in the Spanish Pyrenees: Special Publication of the International Association of Sedimentologists, v. 28, p. 221–230.
British Geological Survey/Department of Public Health Engineering (BGS/DPHE) Reports, 2001, Arsenic contamination of groundwater in Bangladesh, *in* Kinniburgh D.G., and Smedley, P., eds., British Geological Survey technical report, WC/00/19: Keyworth, British Geological Survey, four volumes.
Cheng, Z., van Geen, A., Seddique, A.A., and Ahmed, K.M., 2005, Limited temporal variability of arsenic concentrations in 20 wells monitored for 3 years in Araihazar, Bangladesh: Environmental Science and Technology, v. 39, no. 13, p. 4759–4766, doi: 10.1021/es048065f.
Cheng, Z., van Geen, A., Rahman, M., Jia, Q., and Matin, K., 2006, Monitoring of arsenic concentrations in groundwater pumped from 50 community wells tapping Pleistocene aquifers in Araihazar, Bangladesh: Geological Society of America Abstracts with Programs, v. 38, no. 7, p. 180.
Clifford, H.T., and Stephenson, W., 1975, An introduction to numerical classification: New York, Academic Press, 229 p.
Coleman, J.M., 1969, Brahmaputra River: Channel processes and sedimentation: Sedimentary Geology, v. 3, no. 2–3, p. 129–239, doi: 10.1016/0037-0738(69)90010-4.
Cutshall, N.H., Larsen, I.L., and Olsen, C.R., 1983, Direct analysis of ^{210}Pb in sediment samples: Self-absorption corrections: Nuclear Instruments and Methods, v. 206, p. 309–312, doi: 10.1016/0167-5087(83)91273-5.
Datta, D.K., and Subramanian, V., 1997, Texture and mineralogy of sediments from the Ganges-Brahmaputra-Meghna river system in the Bengal Basin, Bangladesh and their environmental implications: Environmental Geology, v. 30, p. 181–188, doi: 10.1007/s002540050145.
Dhar, R., 2006, Arsenic and groundwater properties of Araihazar, Bangladesh [Ph.D. thesis]: Queens College, City University of New York, 192 p.
Fergusson, J., 1863, On recent changes in the delta of the Ganges: London, Quarterly Journal of the Geological Society, v. 19, p. 321–354.
Goodbred, S.L., and Kuehl, S.A., 1998, Floodplain processes in the Bengal Basin and the storage of Ganges-Brahmaputra sediment: An accretion study using ^{137}Cs and ^{210}Pb geochronology: Sedimentary Geology, v. 121, p. 239–258, doi: 10.1016/S0037-0738(98)00082-7.
Goodbred, S.L., and Kuehl, S.A., 2000, The significance of large sediment supply, active tectonism, and eustasy on margin sequence development: Late Quaternary stratigraphy and evolution of the Ganges-Brahmaputra delta: Sedimentary Geology, v. 133, p. 227–248, doi: 10.1016/S0037-0738(00)00041-5.
Harvey, C.F., Swartz, C.H., Badruzzaman, A.B.M., Keon-Blute, N., Yu, W., Ali, M.A., Jay, J., Beckie, R., Niedan, V., Brabander, D., Oates, P.M., Ashfaque, K.N., Islam, S., Hemond, H.F., and Ahmed, M.F., 2002, Arsenic mobility and groundwater extraction in Bangladesh: Science, v. 298, p. 1602–1606, doi: 10.1126/science.1076978.
He, Q., and Walling, E., 1996, Use of fallout Pb-210 measurements to investigate longer-term rates and patterns of overbank sediment deposition on the floodplains of lowland rivers: Earth Surface Processes and Landforms, v. 21, p. 141–154, doi: 10.1002/(SICI)1096-9837(199602)21:2<141:AID-ESP572>3.0.CO;2-9.
Hickin, E.J., 1974, Development of meanders in natural river channels: American Journal of Science, v. 274, no. 4, p. 414–442.
Horneman, A., van Geen, A., Kent, D., Mathe, P.E., Zheng, Y., Dhar, R.K., O'Connell, S., Hoque, M., Aziz, Z., Shamsudduha, M., Seddique, A., and Ahmed, K.M., 2004, Decoupling of arsenic and iron release to Bangladesh groundwater under reducing conditions. Part I: Evidence from sediment profiles: Geochimica et Cosmochimica Acta, v. 68, no. 17, p. 3459–3473, doi: 10.1016/j.gca.2004.01.026.
Ingebritsen, S.E., and Sanford, W.E., 1998, Groundwater in geologic processes: New York, Cambridge University Press, 562 p.
Jain, M., Tandon, S.K., Bhatt, S.C., Singhvi, A.K., and Mishra, S., 1999, Alluvial and aeolian sequences along the River Luni, Barmer District: Physical stratigraphy and feasibility of luminescence chronology methods, *in* Radhakrishna, B.P., and Merh, S.S., eds., Memoir: Vadodara, Geological Society of India, p. 273–295.
Kale, V.S., Singhvi, A.K., Mishra, P.K., and Banerjee, D., 2000, Sedimentary records and luminescence chronology of late Holocene pelaeofloods in the Luni River, Thar Desert, Northwest India: Catena (Giessen), v. 40, no. 4, p. 337–358.
Lamy, F., Hebbeln, D., and Wefer, G., 1998, Late Quaternary precessional cycles of terrigenous sediment input off the Norte Chico, Chile (27.5°S) and palaeoclimatic implications: Palaeogeography, Palaeoclimatology, Palaeoecology, v. 141, no. 3–4, p. 233–251, doi: 10.1016/S0031-0182(98)90052-9.
Liu, C.-W., Jang, C.-S., and Liao, C.-M., 2004, Evaluation of arsenic contamination potential using indicator kriging in the Yun-Lin aquifer (Taiwan): The Science of the Total Environment, v. 321, no. 1–3, p. 173–188, doi: 10.1016/j.scitotenv.2003.09.002.
McArthur, J.M., Banerjee, D.M., Hudson-Edwards, K.A., Mishra, R., Purohit, R., Ravenscroft, P., Cronin, A., Howarth, R.J., Chatterjee, A., Talukder, T., Lowry, D., Houghton, S., and Chadha, D.K., 2004, Natural organic matter in sedimentary basins and its relation to arsenic in anoxic groundwater: The example of West Bengal and its worldwide implications: Applied Geochemistry, v. 19, p. 1255–1293, doi: 10.1016/j.apgeochem.2004.02.001.
Meharg, A.A., Scrimgeour, C., Hossain, S.A., Fuller, K., Cruickshank, K., Williams, P.N., and Kinniburgh, D.G., 2006, Codeposition of organic carbon and arsenic in Bengal Delta aquifers: Environmental Science and Technology, v. 40, p. 4928–4935, doi: 10.1021/es060722b.
Murray, A.S., and Wintle, A.G., 2000, Luminescence dating of quartz using an improved single-aliquot regenerative-dose protocol: Radiation Measurements, v. 32, p. 57–73, doi: 10.1016/S1350-4487(99)00253-X.
Nickson, R.T., McArthur, J.M., Ravenscroft, P., Burgess, W.G., and Ahmed, K.M., 2000, Mechanism of arsenic release to groundwater, Bangladesh and West Bengal: Applied Geochemistry, v. 15, p. 403–413, doi: 10.1016/S0883-2927(99)00086-4.
Prescott, J.R., and Hutton, J.T., 1988, Cosmic ray and gamma ray dosimetry for TL and ESR: Nuclear Tracks and Radiation Measurements, v. 14, p. 223–227, doi: 10.1016/1359-0189(88)90069-6.
Radloff, K.A., Cheng, Z.Q., Rahman, M.W., Ahmed, K.M., Mailloux, B.J., Juhl, A.R., Schlosser, P., and van Geen, A., 2007, Mobilization of arsenic during one-year incubations of grey aquifer sands from Araihazar, Bangladesh: Environmental Science and Technology, v. 41, no. 10, p. 3639–3645, doi: 10.1021/es062903j.
Rasid, H., 1966, Morphology of the Jamuna floodplains: The Oriental Geographer, v. 10, no. 2, p. 57–72.
Ravenscroft, P., Burgess, W.G., Ahmed, K.M., Burren, M., and Perrin, J., 2005, Arsenic in groundwater of the Bengal Basin, Bangladesh: Distribution, field relations, and hydrogeological setting: Hydrogeology Journal, v. 13, p. 727–751, doi: 10.1007/s10040-003-0314-0.
Sandberg, S.K., Slater, L.D., and Versteeg, R., 2002, An integrated geophysical investigation of the hydrogeology of an anisotropic unconfined aquifer: Journal of Hydrology, v. 267, no. 3–4, p. 227–243, doi: 10.1016/S0022-1694(02)00153-1.
Sengupta, S., Mukherjee, P.K., Pal, T., and Shome, S., 2004, Nature and origin of arsenic carriers in shallow aquifer sediments of Bengal Delta, India: Environmental Geology, v. 45, p. 1071–1081, doi: 10.1007/s00254-004-0965-8.
Smedley, P.L., Zhang, M., Zhang, G., and Luo, Z., 2003, Mobilization of arsenic and other trace metals in fluviolacustrine aquifers of the Huhhot Basin, Inner Mongolia: Applied Geochemistry, v. 18, p. 1453–1477, doi: 10.1016/S0883-2927(03)00062-3.
Srivastava, P., Juyal, N., Singhvi, A.K., Wasson, R.J., and Bateman, M.D., 2001, Luminescence chronology of river adjustment and incision of Quaternary sediments in the alluvial plain of the Sabarmati River, north Gujarat, India: Geomorphology, v. 36, p. 217–229, doi: 10.1016/S0169-555X(00)00058-1.
Stute, M., Zheng, Y., Schlosser, P., Horneman, A., Dhar, R.K., Hoque, M.A., Seddique, A.A., Shamsudduha, M., Ahmed, K.M., and van Geen, A., 2007, Hydrological control of As concentrations in Bangladesh groundwater: Water Resources Research, v. 43, p. W09417, doi: 10.1029/2005WR004499
Suiling, W., and Mulligan, C.N., 2006, Natural attenuation processes for remediation of arsenic contaminated soils and groundwater: Journal of Hazardous Materials, v. 138, p. 459–470.
van Geen, A., Ahsan, H., Horneman, A.H., Dhar, R.K., Zheng, Y., Hussain, I., Ahmed, K.M., Gelman, A., Stute, M., Simpson, H.J., Wallace, S., Small, C., Parvex, F., Slavkovich, V., Lolacono, N.J., Becker, M., Cheng, Z., Momotaj, H., Shahnewaz, M., Seddique, A.A., and Graziano, J.H., 2002, Promotion of well-switching to mitigate the current arsenic crisis in Bangladesh: Bulletin of the World Health Organization, v. 80, p. 732–737.
van Geen, A., Zheng, Y., Versteeg, R., Stute, M., Horneman, A., Dhar, R., Steckler, M., Gelman, A., Small, C., Ahsan, H., Graziano, J.H., Hussain, I., and Ahmed, K.M., 2003, Spatial variability of arsenic in 6000 tube wells in a 25 km^2 area of Bangladesh: Water Resources Research, v. 39, no. 5, p. 1140, doi: 10.1029/2002WR001617.
van Geen, A., Protus, T., Cheng, Z., Horneman, A., Seddique, A.A., Hoque, M.A., and Ahmed, M., 2004, Testing groundwater for arsenic in Bangladesh before installing a well: Environmental Science and Technology, v. 38, no. 24, p. 6783–6789, doi: 10.1021/es049323b.
van Geen, A., Aziz, Z., Horneman, A., Weinman, B., Dhar, R.K., Zheng, Y., Goodbred, S., Versteeg, R., Seddique, A.A., Hoque, M.A., and Ahmed, K.M., 2006a, Preliminary evidence of a link between surface soils properties and the arsenic content of shallow groundwater in Bangladesh: Journal of Geochemical Exploration, v. 88, p. 157–161, doi: 10.1016/j.gexplo.2005.08.106.
van Geen, A., Trevisani, M., Immel, J., Jakariya, M., Osman, N., Cheng, Z., Gelman, A., and Ahmed, K.M., 2006b, Targeting low-arsenic groundwater with mobile-phone technology in Araihazar, Bangladesh: Journal of Health, Population, and Nutrition, v. 24, no. 3, p. 282–297.
van Geen, A., Zheng, Y., Cheng, Z., Aziz, Z., Horneman, A., Dhar, R.K., Mailloux, B., Stute, M., Weinman, B., Goodbred, S., Seddique, A.A., Hope, M.A., and Ahmed, K.M., 2006c, A transect of groundwater and sediment properties in Araihazar, Bangladesh: Further evidence of decoupling between As and Fe mobilization: Chemical Geology, v. 228, no. 1–3, p. 85–96.
von Brömssen, M., Jakariya, M., Bhattacharya, P., Ahmed, K.M., Hasan, M.A., Sracek, O., Jonsson, L., Lundell, L., and Jacks, G., 2007, Targeting low-arsenic aquifers in Matlab Upazila, southeastern Bangladesh: Science of the Total Environment, v. 379, no. 2–3, p. 121–132, doi: 10.1016/j.scitotenv.2006.06.028.
Yu, W.H., Harvey, C.M., and Harvey, C.F., 2003, Arsenic in groundwater in Bangladesh: A geostatistical and epidemiological framework for evaluating health effects and potential remedies: Water Resources Research, v. 39, no. 6, p. 1146, doi: 10.1029/2002WR001327.
Zheng, Y., van Geen, A., Stute, M., Dhar, R., Mo, Z., Cheng, Z., Horneman, A., Gavrieli, I., Simpson, H.J., Versteeg, R., Steckler, M., Goodbred, S., Ahmed, K.M., Shanewaz, M., and Shamsudduha, M., 2005, Contrast in groundwater arsenic in shallow Holocene and older deep aquifers: A case study in two villages of Araihazar, Bangladesh: Geochimica et Cosmochimica Acta, v. 69, no. 22, p. 5203–5218, doi: 10.1016/j.gca.2005.06.001.

Manuscript received 25 February 2007
Revised manuscript received 1 October 2007
Manuscript accepted 9 October 2007

Printed in the USA